Importance of voltage-dependent inactivation in N-type calcium channel regulation by G-proteins

Weiss Norbert [1] , Tadmouri Abir [1] , Mikati Mohamad [2] , Ronjat Michel [1] , De Waard Michel [1 *]

[1] Canaux calciques , fonctions et pathologies INSERM : U607, CEA : DSV/IRTSV, Université Joseph Fourier - Grenoble I, 17, rue des martyrs 38054 Grenoble,FR

[2] Department of Pediatrics American University of Beirut Medical Center, Beyrouth,LB

* Correspondence should be adressed to: Michel De Waard <michel.dewaard@ujf-grenoble.fr>

Abstract

Direct regulation of N-type calcium channels by G-proteins is essential to control neuronal excitability and neurotransmitter release. Binding of the $G_{\beta\gamma}$ dimer directly onto the channel is characterized by a marked current inhibition ("ON" effect), whereas the pore opening- and time-dependent dissociation of this complex from the channel produce a characteristic set of biophysical modifications ("OFF" effects). Although G-protein dissociation is linked to channel opening, the contribution of channel inactivation to G-protein regulation has been poorly studied. Here, the role of channel inactivation was assessed by examining time-dependent G-protein de-inhibition of $Ca_v2.2$ channels in the presence of various inactivation-altering β subunit constructs. G-protein activation was produced via μ-opioid receptor activation using the DAMGO agonist. Whereas the "ON" effect of G-protein regulation is independent of the type of β subunit, the "OFF" effects were critically affected by channel inactivation. Channel inactivation acts as a synergistic factor to channel activation for the speed of G-protein dissociation. However, fast inactivating channels also reduce the temporal window of opportunity for G-protein dissociation, resulting in a reduced extent of current recovery, whereas slow inactivating channels undergo a far more complete recovery from inhibition. Taken together, these results provide novel insights on the role of channel inactivation in N-type channel regulation by G-proteins and contribute to the understanding of the physiological consequence of channel inactivation in the modulation of synaptic activity by G-protein coupled receptors.

MESH Keywords Animals ; Calcium Channels, N-Type ; metabolism ; physiology ; Electric Conductivity ; Electrophysiology ; GTP-Binding Proteins ; metabolism ; physiology ; Kinetics ; Protein Isoforms ; metabolism ; physiology ; Rabbits ; Rats ; Receptors, Opioid, mu ; physiology ; Time Factors

Author Keywords N-type calcium channel ; Cav2.2 subunit ; G-protein ; G-protein coupled receptor ; μ-opioid receptor ; inactivation ; beta subunit.

Introduction

Voltage-dependent N-type calcium channels play a crucial role in neurotransmitter release at central and peripheral synapse (3, 47). Several subtypes of N-type channels are known to exist that differ in their inactivation properties either because of differences in subunit composition (43) or because they represent splice variants (5, 28). N-type channels are strongly regulated by G-protein coupled receptors (GPCRs) (4, 18, 25, 29, 30). Direct regulation by G-proteins involves the binding of the $G_{\beta\gamma}$ dimer (22, 27) on various structural determinants of $Ca_v2.2$, the pore-forming subunit of N-type channels (1, 12, 15, 23, 33, 38, 44, 53). This regulation is characterized by typical biophysical modifications of channel properties (14), including: i) a marked current inhibition (7, 51), ii) a slowing of activation kinetics (30), iii) a depolarizing shift of the voltage-dependence of activation (4), iv) a current facilitation following prepulse depolarization (26, 42), and v) a modification of inactivation kinetics (52). Current inhibition has been attributed to $G_{\beta\gamma}$ binding onto the channel ("ON" effect), whereas all other channel modifications are a consequence of a variable time-dependent dissociation of $G_{\beta\gamma}$ from the channel ("OFF" effects) (48). Although the dissociation of $G_{\beta\gamma}$ was previously described as voltage-dependent (17), it was then suggested that channel opening following membrane depolarisation was more likely responsible for the removal of $G_{\beta\gamma}$ (35). More recently, we have shown that the voltage-dependence of the time constant of $G_{\beta\gamma}$ dissociation was directly correlated to the voltage-dependence of channel activation suggesting that $G_{\beta\gamma}$ dissociation is in fact intrinsically voltage-independent (48).

Although $G_{\beta\gamma}$ dissociation, and the resultant characteristic biophysical changes associated with it, has been correlated with channel activation, the contribution of channel inactivation in G-protein regulation has been barely studied. Evidence that such a link may exist has emerged from a pioneering study from the group of Prof. Catterall (23) in which it was demonstrated that mutations of the β subunit binding domain of $Ca_v2.1$, known to affect inactivation, also modify G-protein modulation. A slower inactivating channel, in which the Arg residue of the QQIER motif of this domain was substituted by Glu, enhanced the prepulse facilitation suggesting that the extent of G-protein dissociation was enhanced. However, establishing a specific relationship between channel inactivation and G-protein regulation with mutants of such a motif is rendered difficult because this motif is also a $G_{\beta\gamma}$ binding determinant (15, 23, 53). Indeed, mutations of this motif are expected to decrease the affinity of G-proteins for the channel, and hence may facilitate G-protein dissociation. Differences in G-protein regulation of $Ca_v2.2$ channels have also been reported if the channel is associated to β subunit that induce different

inactivation kinetics (11, 20, 31). However, in none of these studies, a formal link between channel inactivation and G-protein regulation has been established.

In this study, we analyzed how modifying channel inactivation kinetics could affect the parameters of G-protein dissociation (time constant and extent of dissociation). We used a method of analysis that was recently developed on N-type channels for extracting all parameters of G-protein regulation at regular potential values, independently of the use of prepulse depolarisations (49). The objective was to perform a study in which the structural properties of the pore-forming subunit would remain unaltered in order to keep the known G-protein binding determinants of the channel functionally intact. Structural analogues of β subunits, known or expected to modify channel inactivation properties, were used (16, 32, 40). It is concluded that fast inactivation accelerates G-protein dissociation from the channel, whereas slow inactivation slows down the process. However, channel inactivation also reduces the temporal window of opportunity in which G-protein dissociation can be observed. Far less recovery is observed for channels that undergo fast inactivation, whereas slow inactivating channels display almost complete G-protein dissociation. With regard to the landmark effects of G-protein regulation, it is concluded that the “ON” effect (extent of G-protein inhibition) is independent of the type of inactivation provided by β subunits, whereas all “OFF” effects (slowing of activation and inactivation kinetics, shift of the voltage-dependence of activation) are largely influenced by the kinetics of channel inactivation induced by the β constructs. These results better explain the major differences that can be observed in the regulation of functionally distinct N-type channels. Furthermore, they provide an insight of the potential influence of channel inactivation in modulating G-protein regulation of N-type channels at the synaptic level.

Materials and Methods

Materials

The cDNAs used in this study were rabbit $Ca_v2.2$ (GenBank accession number D14157), rat β_{1b} (X61394), rat β_{2a} (M80545), rat β_3 (M88751), rat β_4 (L02315) and rat μ-opioid receptor (rMOR, provided by Dr. Charnet). D-Ala^2, Me-Phe^4, glycinol^5)-Enkephalin (DAMGO) was from Bachem (Bubendorf, Germany).

Molecular biology

The CD8-β_{1b} chimera was generated by polymerase chain reaction (PCR) amplification of the full length β_{1b} using oligonucleotide primers 5′-CGCGGATCCGTCCAGAAGAGCGGCATGTCCCGGGGCCCTTACCCA-3′ (forward) and 5′ -ACGTGAATTCGCGGATGTAGACGCCTTGTCCCCAGCCCTCCAG-3′ (reverse) and the PCR product was subcloned into the BamHI and EcoRI sites of the pcDNA3-CD8-βARK-myc vector after removing the βARK insert (vector generously provided by D. Lang, Geneva University, Geneva, Switzerland). The truncated N-terminal β_{1b} construct ($\beta_{1b\ \Delta N}$, coding for amino acid residues 58 to 597) was performed as described above using the primers 5′ -CGCGGATCCACCATGGGCTCAGCAGAGTCCTACACGAGCCGGCCGTCAGAC-3′ (forward) and 5′ -CGGGGTACCGCGGATGTAGACGCCTTGTCCCCAGCCCTCCAGCTC-3′ (reverse) and the PCR product was subcloned into the Kpn I and BamHI sites of the pcDNA3.1(-) vector (Invitrogen). The truncated N-terminal β_3 construct ($\beta_{3\ \Delta N}$, coding for amino acid residues 16 to 484) was performed using the primers 5′-CGCGGATCCACCATGGGTTCAGCCGACTCCTACACCAGCCGCCCCTCTCTGGAC-3′ (forward) and 5′-CGGGGTACCGTAGCTGTCTTTAGGCCAAGGCCGGTTACGCTGCCAGTT-3′ (reverse) and the PCR product was subcloned into the KpnI and BamHI sites of the pcDNA3.1(-) vector.

Transient expression in Xenopus oocytes

Stage V and VI oocytes were surgically removed from anesthetized adult Xenopus laevis and treated for 2–3 h with 2 mg/ml collagenase type 1A (Sigma). Injection into the cytoplasm of cells was performed with 46 nl of various cRNA mixture in vitro transcribed using the SP6 or T7 mMessage mMachine Kit (Ambion, Cambridgeshire, UK) (0.3 μg/μl $Ca_v2.2$ + 0.3 μg/μl μ-opioid receptor + 0.1 μg/μl of one of the different calcium channel β constructs. Cells were incubated at 19°C in defined nutrient oocyte medium as described (19).

Electrophysiological recording

After incubation for 2–4 days, macroscopic currents were recorded at room temperature (22–24°C) using two-electrode voltage-clamp in a bathing medium containing (in mM): $Ba(OH)_2$ 40, NaOH 50, KCl 3, HEPES 10, niflumic acid 0.5, pH 7.4 with methanesulfonic acid. Electrodes filled with (in mM): KCl 140, EGTA 10 and HEPES 10 (pH 7.2) had resistances between 0.5 and 1 MΩ. Macroscopic currents were recorded using Digidata 1322A and GeneClamp 500B amplifier (Axon Instruments, Union City, CA). Acquisition and analyses were performed using the pClamp 8 software (Axon Instruments). Recording were filtered at 2 kHz. Leak current subtraction was performed on-line by a P/4 procedure. DAMGO was applied at 10 μM by superfusion of the cells at 1 ml/min. All recordings were performed within 1 min after DAMGO produced maximal current inhibition. We observed that this procedure fully minimized voltage-independent G-protein regulation that took place later, 5–10 min after DAMGO application (data not shown). Hence, the inhibition by DAMGO was fully reversible as assessed by washout experiments. Also, no run-down was observed during the time course of these experiments. Cells that presented signs of prepulse facilitation before μ-opioid receptor activation (tonic inhibition) were discarded from the analyses.

Analyses of the parameters of G-protein regulation

The method used to extract all biophysical parameters of G-protein regulation (GI_{t_0}, the initial extent of G-protein inhibition before the start of depolarisation, τ, the time constant of G-protein unbinding from the channel, and RI, the extent of recovery from inhibition at the end of a 500 ms test pulse, unless specified in the text) were described elsewhere (49). The key steps required to extract these parameters are briefly summarized in Fig. 1. This method is analogous to the method that relies on the use of prepulses but avoids many of the pitfalls of the latter (use of an interpulse potential that favours G-protein reassociation, differences in the rate of channel inactivation between control and G-protein regulated channels, and facilitation that occurs during the control test pulse) (49).

Mathematical and statistical analyses

Current-voltage relationships (I/V) were fitted with the modified Boltzmann equation $I_{(V)} = G_{max} \times (V-E))/(1+\exp(-(V-V_{1/2})/k))$ where $I_{(V)}$ represents the maximal current amplitude in response to a depolarisation at the potential V, G_{max} the maximal conductance, E the inversion potential of the Ba^{2+}, and k a slope factor. All data are given as mean ± S.E.M for n number observations and statistical significance (p) was calculated using Student's t-test. Statistical significance for scatter plot analysis was performed using the Spearman Rank Order correlation test.

Results

N-type current inhibition by G-proteins is independent of the β subunit species

G-protein inhibition is generally studied through the measurement of the peak currents. However, this approach doesn't take into account the fact that, at the time to peak, a considerable proportion of G-proteins has already dissociated from the channel during depolarization. In order to better estimate the real extent of N-type current inhibition by G-proteins, we used the technical approach described in Fig. 1 to measure GI_{t_0}, the maximum extent of G-protein inhibition before the start of the G-protein unbinding process. Representative current inhibition and kinetic alterations are shown for $Ca_v2.2$ channels co-expressed with either β_{1b}, β_{2a}, β_3 or β_4 subunit (Fig. 2a, top panel) and the corresponding GI_{t_0} values were quantified (Fig. 2a, bottom panel). The β subunits did not alter significantly the maximum extents of inhibition that ranged between 59.2 ± 1.4% ($Ca_v2.2/\beta_{2a}$ channels, n = 25) and 62.4 ± 1.8% ($Ca_v2.2/\beta_{1b}$ channels, n = 25) (Fig. 2b). In the following part of this study, three other β subunit constructs have been coexpressed with $Ca_v2.2$, $\beta_{1b\,\Delta N}$, CD8-β_{1b} and $\beta_{3\,\Delta N}$. As for the wild-type β isoforms, GI_{t_0} varied non significantly ($p > 0.05$) between 58.4 ± 1.8% ($\beta_{1b\,\Delta N}$, n = 9) and 63.5 ± 1.3 (CD8-β_{1b}, n = 10).

The two parameters that are relevant for the "OFF" effects, τ (the time constant of G-protein unbinding from the channel) and RI (the extent of current recovery from G-protein inhibition after a 500 ms depolarisation), will be used to investigate the role of N-type channel inactivation in G-protein regulation. GI_{t_0} is not a time-dependent parameter and cannot be influenced by the time course of inactivation.

Current recovery from G-protein inhibition is altered when the inactivation kinetics of $Ca_v2.2$ channels are modulated by β subunits

Auxiliary β subunits are known to influence the inactivation kinetics of $Ca_v2.2$ channels with a rank order of potency, from the fastest to the slowest, of $\beta_3 \geq \beta_4 > \beta_{1b} \gg \beta_{2a}$ (45). Representative control current traces at 10 mV for $Ca_v2.2$ channels co-expressed with each type of β-subunits are shown in Fig. 3a (left panel). As expected from former reports, the β_3 subunit produces the fastest inactivation, whereas β_{2a} induced the slowest inactivation. The β_{1b} and β_4 subunits induce intermediate inactivation kinetics. In agreement with previous reports (11, 20), β subunits markedly affect G-protein regulation. Here, we investigated how channel inactivation affects the kinetic of G-protein departure from the channel, as well as the extent of relief from inhibition (RI). The time constants τ of G-protein dissociation were extracted from the $I_{\text{G-proteins unbinding}}$ traces for each combination of channels (Fig. 3a, middle panel), whereas RI was calculated as the extent of dissociation by comparing the current levels of I_{DAMGO}, $I_{DAMGO\ wo\ unbinding}$ and $I_{Control}$ after 500 ms of depolarisation (Fig. 3a, right panel). The data show that both τ and RI values are differentially affected by the kinetics of channel inactivation. Average parameters are reported in Fig. 3b (for τ) and Fig. 3c (for RI). The time constant τ of recovery from G-protein inhibition is 2.9-fold faster for the fastest inactivating channel ($Ca_v2.2/\beta_3$, 37.5 ± 3.3 ms, n = 13) than the slowest inactivating channel ($Ca_v2.2/\beta_{2a}$, 107.8 ± 2.7 ms, n = 22). Interestingly, the rank order for the speed of recovery from G-protein inhibition ($\beta_3 \geq \beta_4 > \beta_{1b} \gg \beta_{2a}$) is similar to that observed for inactivation kinetics. Indeed, student t-tests demonstrate that differences between β subunits are all highly statistically significant ($p \leq 0.001$) except between β_3 and β_4 were the difference is less pronounced ($p \leq 0.05$) (Fig. 3b). It is thus concluded that the speed of channel inactivation imposed by each type of β subunit impacts the time constant of recovery from G-protein inhibition. Channel inactivation appears as a "synergistic factor" to channel activation (48) for the speed of G-protein dissociation. Next, the effects of β subunits were investigated on RI values (Fig. 3c). Two of the β subunits (β_3 and β_4) have closely related RI values (56.9 ± 1.8% (n = 21) vs 56.8 ± 1.2% (n = 34)). In contrast, β_{1b} and β_{2a} statistically decrease (45.0 ± 1.3%, n = 24) and increase (96.1 ± 1.4%, n = 29) RI values, respectively. From these data, it is clear that faster recovery from inhibition is not necessarily associated with an elevated RI value. Although channel

inactivation accelerates the kinetics of G-protein dissociation from the channel, it also reduces the time window in which the process can be completed. In these data, a relationship seems to exist between channel inactivation conferred by β subunits and G-protein dissociation. It is however unclear whether this link is only due to the kinetics of inactivation conferred by β subunits or also to differences in molecular identities. In order to precise these first observation, we examined how structural modifications of individual β subunits, known to alter channel inactivation, affect the recovery parameters from G-protein inhibition.

Deletion of a β subunit determinant important for fast inactivation alters recovery from G-protein inhibition

Important determinants for the control of inactivation rate have been identified in the past on β subunits (32, 37). Deletion of the amino-terminus of β subunits is known to slow-down channel inactivation (16). According to the data of Fig. 3, slowing of inactivation should increase both the time constant τ of recovery from G-protein inhibition and the extent of recovery RI. Fig. 4a & b illustrate the extent of slowing in inactivation kinetics of $Ca_v2.2/\beta_{1b}$ channels when the first N-terminal 57 amino acids of β_{1b} subunit are deleted ($\beta_{1b\,\Delta N}$). The amount of inactivation at the end of a 500 ms depolarization at 10 mV shows a 2.2-fold decrease from 58.4 ± 1.6% (n = 22) to 26.2 ± 2.3% (n = 10) (Fig. 4b). Representative traces of DAMGO regulation of $Ca_v2.2/\beta_{1b}$ and $Ca_v2.2/\beta_{1b\,\Delta N}$ currents demonstrate that the deletion of the N-terminus of β_{1b} produces a significant modification in G-protein regulation (Fig. 4c, left panel). Notably, DAMGO-inhibited $Ca_v2.2/\beta_{1b\,\Delta N}$ currents display much slower activation kinetics (quantified in Fig. 8c). The analysis of the time-course of $I_{G\text{-proteins unbinding}}$ traces in the presence of truncated β_{1b} reveals a slower time-course (Fig. 4c, middle panel). Also, the deletion of the N-terminus of β_{1b} leads to an increased recovery from G-protein inhibition (Fig. 4c, right panel). Statistical analyses show a significant increase in the time constant τ of recovery (2.0-fold) from 60.0 ± 2.0 ms (n = 24) to 118.6 ± 2.5 ms (n = 10) (Fig. 4d) and an increase in the RI values (1.8-fold) from 45.0 ± 1.3% (n = 24) to 79.6 ± 2.5% (n = 9) by the deletion of the N-terminus of β_{1b} (Fig. 4e).

To confirm that these effects are independent of the nature of the β subunit involved, similar experiments were conducted with a 15 amino acid N-terminal truncated β_3 subunit ($\beta_{3\,\Delta N}$). As for $\beta_{1b\,\Delta N}$, $\beta_{3\,\Delta N}$ produces a slowing of channel inactivation kinetics. After 500 ms at 10 mV, $Ca_v2.2/\beta_3$ channels inactivate by 68.9 ± 1.7% (n = 21) compared to 41.1 ± 1.1% (n = 10) for $Ca_v2.2/\beta_{3\,\Delta N}$ channels (Fig. 5a,b). As expected, DAMGO inhibition of $Ca_v2.2/\beta_{3\,\Delta N}$ channels produces currents with slower activation and inactivation kinetics than $Ca_v2.2/\beta_3$ channels (shift of the time to peak of the current from 20.7 ± 2.5 ms with β_3 (n = 21) to 77.0 ± 7.6 ms with $\beta_{3\,\Delta N}$ (n = 10) (Fig. 5c, left panel). Moreover, the time course of $I_{G\text{-proteins unbinding}}$ was slowed-down with the N-terminal truncation of β_3 (Fig. 5c, middle panel), and the recovery from inhibition was enhanced (Fig. 5c, right panel). Quantification of these effects reveals a statistically significant slowing (1.8-fold) of the time constant of recovery τ from G-protein inhibition from 37.5 ± 3.3 ms (n = 13) to 67.4 ± 4.5 ms (n = 10) (Fig. 5d) and an increase of RI values (1.2-fold) from 56.9 ± 1.8% (n = 21) to 66.9 ± 2.1% (n = 10). However, the time constant of recovery in the presence of $\beta_{3\,\Delta N}$ remains fast compared to the inactivation kinetics, which may explain the lower increase in RI values compared to what has been measured with $\beta_{1b\,\Delta N}$. Also, the starting value of RI is high for β_3 (56.9%) compared to β_{1b} (45.0%) which limits the possibility of increase.

Slowing of channel inactivation by membrane anchoring of β subunit also alters the properties of recovery from G-protein inhibition

Another approach to modulate channel inactivation is to modify the docking of the β subunits to the plasma membrane (13, 40). For that purpose, we expressed a membrane-inserted CD8 linked to β_{1b} subunit (CD8-β_{1b}) along with $Ca_v2.2$. As shown in earlier studies using the same strategy but with a different β subunit (2, 40), membrane anchoring of β_{1b} subunit significantly slows down the inactivation kinetics (Fig. 6a). Indeed, inactivation was reduced by 1.5-fold from 58.4 ± 1.6% (n=22) to 38.1 ± 1.8% (n=10) (Fig. 6b). Membrane anchoring of β_{1b} via CD8 slowed down the DAMGO inhibited current activation kinetics (Fig. 6c, left panel). Under DAMGO inhibition, a greater shift of the time to peak of the current was observed for CD8-β_{1b} than for β_{1b} (from 57.0 ± 4.1 ms with β_{1b} (n = 12) to 168.8 ± 7.0 ms with CD8-β_{1b} (n = 10)). Also, recovery from inhibition was slowed 1.9-fold from 60.0 ± 2.0 ms (n = 24) to 112.3 ± 5.4 ms (n = 8) (Fig. 6d), whereas RI increased 1.3-fold from 45.0 ± 1.3% (n = 24) to 58.0 ± 1.9% (n = 9).

Inactivation limits the maximum observable recovery from G-protein inhibition

As demonstrated above, inactivation influences both the time constant of recovery and the maximal observable recovery from inhibition. In order to study the effect of channel inactivation on the maximum recovery from inhibition, independently of the time constant of recovery, we compared RI values and inactivation at a fixed time constant of recovery. The time constant of recovery from inhibition shows a voltage-dependence similar to that of channel opening (48). An example of this voltage-dependence is illustrated in Fig. 7a (left panel) for $Ca_v2.2/\beta_{1b}$ channels. A plot of the time constant of recovery as a function of membrane depolarization indicates a great extent of variation in τ values (Figure 7a, middle panel). This voltage-dependency of τ values was observed for all channel combinations (data not shown). We then chose to impose the τ value to 50 ± 5 ms for all expressed channel combinations by selecting the appropriate recordings from the set of traces obtained at various test potentials (Fig. 7a, right panel). This τ value was chosen because it allows the incorporation of a large number of recordings in the analysis. Also, with a τ of 50 ms, the RI value at 500 ms after depolarisation has

reached saturation (95% of recovery after 150 ms of depolarisation). For traces that underwent a recovery from inhibition with a τ value of 50 ± 5 ms, we measured the extent of recovery RI and of inactivation, both at 500 ms. Representative examples for different channel combinations ($Ca_v2.2$ along with either β_{2a}, β_4 or β_3, from the slowest to the fastest inactivation) are shown in Fig. 7b (left panel) where the RI values and the extent of inactivation (right panel) are measured in each experimental condition. Fig. 7c shows the negative correlation existing between the extent of maximum recovery from inhibition and the extent of inactivation (statistically significant at $p < 0.001$, $n = 62$). These results demonstrate that the only restriction to observe a complete current recovery from G-protein inhibition is the inactivation process. Indeed, channels that have almost no inactivation ($Ca_v2.2/\beta_{2a}$) show a complete recovery from inhibition. The curve predicts that, for completely non-inactivating channels, 100% of the current would recover from inhibition. These results confirm that the experimental protocol used herein to minimize voltage-independent inhibition was fully functional. Conversely, channels that present the most inactivation present the smallest amount of recovery from inhibition.

Differences in calcium channel inactivation generate drastic differences in the biophysical characteristics of G-protein regulation

Since recovery from G-protein inhibition induces an apparent slowing of activation and inactivation kinetics and shifts the voltage-dependence of activation towards depolarized values (48), differences in channel inactivation that affect the recovery process should also affect the biophysical effects of G-proteins on N-type channels. Calcium currents are generally measured at peak amplitudes. The consequences of this protocol are shown for $Ca_v2.2/\beta_{1b}$ and $Ca_v2.2/\beta_{1b\,\Delta N}$ channels that present different inactivation kinetics (Fig. 8a,b). Several observations can be raised. First, it is observed that the slowing of $Ca_v2.2$ inactivation induced by truncating the N-terminus of β_{1b} is responsible for a drastic slowing of activation kinetics under DAMGO application. This effect is most pronounced at low potential values and is significantly reduced at high potential values. These effects are quantified in Fig. 8c. For instance, at 0 mV, the average shift of the time to peak for $Ca_v2.2/\beta_{1b\,\Delta N}$ channels (307.7 ± 9.0 ms, $n = 10$) is on average 9.2-fold greater than that observed for $Ca_v2.2/\beta_{1b}$ channels (33.4 ± 5.2 ms, $n = 19$) (Fig. 8c). Differences in slowing of activation kinetics, triggered by the two β subunits, remain statistically significant for potential values up to 30 mV. Above 30 mV, the convergence of both curves can be explained by the fact that recovery from G-protein inhibition becomes too rapid to be influenced by changes in inactivation kinetics. Second, at the time points of the peak of the current, slowing of inactivation by the N-terminal truncation of β_{1b} induces i) an hyperpolarising shift of the voltage-dependence of RI_{peak} values, and ii) an increase in RI_{peak} values for potentials equal or below 30 mV (Fig. 8d). Since RI_{peak} values represent a voltage-dependent gain of current that is added to the unblocked fraction of control currents under G-protein regulation, they apparently modify the voltage-dependence of channel activation (I/V curves) and reduce the level of DAMGO inhibition (48). For $Ca_v2.2/\beta_{1b}$ channels, average half-activation potential values were significantly shifted by 6.4 ± 0.9 mV (n=13) under DAMGO inhibition, whereas for $Ca_v2.2/\beta_{1b\,\Delta N}$ channels, a non significant shift by 1.9 ± 0.5 mV (n=10) was determined (Fig. 8e,f). This difference in behaviour can readily be explained by the voltage-dependence of RI_{peak} values. In the case of $Ca_v2.2/\beta_{1b}$, the maximal RI_{peak} occurs at 30 mV (Fig. 8d), a depolarizing shift of 20 mV compared to control $Ca_v2.2/\beta_{1b}$ currents, which is responsible for the depolarizing shift of the I/V curve under DAMGO inhibition (Fig. 8e). Conversely, for $Ca_v2.2/\beta_{1b\,\Delta N}$, the maximal RI_{peak} value is observed at 10 mV (Fig. 8d), which is −5 mV hyperpolarized to the control $Ca_v2.2/\beta_{1b\,\Delta N}$ peak currents, and therefore influences far less the I/V curve under DAMGO inhibition (Fig. 8f). Finally, it should be noted that with a slowing of inactivation kinetics, the resultant increase in RI_{peak} values (Fig. 8d, for potentials below 40 mV) produces an apparent reduction in DAMGO inhibition that is clearly evident when one compares the effect of DAMGO on I/V curves of $Ca_v2.2/\beta_{1b}$ and $Ca_v2.2/\beta_{1b\,\Delta N}$ (Fig. 8e,f).

In conclusion, these data indicate that slowing of channel inactivation kinetics increases the slowing of the time to peak by DAMGO, whereas it reduces both the peak current inhibition and the depolarizing shift of the voltage-dependence of activation.

Discussion

Relevant parameters to study the influence of inactivation on N-type channel regulation by G-proteins

N-type channel regulation by G-proteins can be described accurately by three parameters: the G-protein inhibition level at the onset of depolarization (GI_{t_0}), the time constant of recovery from inhibition (τ), and the maximal extent of recovery from inhibition (RI). GI_{t_0} is indicative of the “ON” effect, whereas τ and RI are the quantitative parameters leading to all “OFF” effects of the G-protein regulation (48). Since GI_{t_0} is a quantitative index of the extent of G-protein inhibition at the start of the depolarization, i.e. at a time point where no inactivation has yet occurred, inactivation cannot influence this parameter. On the other hand, G-protein dissociation is a time-dependent process at any given membrane potential and can be thus affected by channel inactivation since both processes occur within a similar time scale. This study aimed at investigating this issue and comes up with two novel conclusions. First, channel inactivation kinetics influences the speed of G-protein dissociation, and second, removal of G-proteins occurs within a time window that is closely controlled by inactivation. Hence, the speed of G-protein dissociation and the time window during which this process may occur control the extent of current recovery from G-protein inhibition at any given time. These conclusions were derived from the use of a recent biophysical method of analysis of N-type calcium channel regulation by G-proteins which is independent of potential changes in channel inactivation behaviour while G-proteins are bound onto the channels (49).

G-protein inhibition is completely reversible during depolarization provided that the channel has slow inactivation

There are two physiological ways to terminate direct G-protein regulation on N-type calcium channels: i) the end of GPCR stimulation by recapture or degradation of the agonist (experimentally mimicked by washout of the bath medium), and ii) membrane depolarization by trains of action potentials (experimentally simulated by a prepulse application). Whereas the first one always leads to a complete recovery from G-protein inhibition, the second one produces a transient and variable recovery. Interestingly, a very slowly inactivating channel, such as the one produced by the combination of $Ca_v2.2$ and β_{2a} subunits, can lead to a complete recovery from G-protein inhibition following membrane depolarisation, whereas a fast inactivating channel such as the one produced by the co-expression of the β_{1b} subunit leads only to a partial recovery. For slow inactivating channels, the time window for G-protein dissociation is large since channel inactivation does not interfere with the process. Conversely, for fast inactivating channels, the time window for G-proteins to unbind from the channel is considerably reduced since inactivation prevents the observation of a complete recovery from inhibition. For these channels, the extent of recovery from inhibition is controlled by both the speed of G-protein dissociation and the time window of opportunity. Hence, the speed of current recovery from G-protein inhibition is controlled by channel inactivation as well as by channel opening as previously shown (48), whereas the time window opportunity of this process is only controlled by channel inactivation. It is likely that both parameters (the time constant of recovery τ and the time window of opportunity) are under the control of additional molecular players or channel modifying agents such as phosphorylation that may act on one or the other parameters in an independent manner, and could contribute to a fine control of the direct G-protein regulation.

There is an unexpected relationship between the channel inactivation kinetics and the kinetics of current recovery from G-protein inhibition

One surprising observation from this study is that fast inactivation accelerates the speed of current recovery from G-protein inhibition, whereas, on the contrary, slower inactivation slows down G-protein dissociation from the channel. This was first demonstrated through the use of different β subunit isoforms (see also (11, 20)), and then confirmed with β subunit constructs known to modify channel inactivation kinetics. Besides this functional correlation, there might be a structural basis that underlies a mechanistic link between channel inactivation and G-protein dissociation. Indeed, (23) illustrated that an R to A mutation of the QXXER motif (one of the $G_{\beta\gamma}$ binding determinant within the I–II linker of $Ca_v2.x$ channels (15)) slows both the inactivation kinetics and the recovery from G-protein inhibition. The I–II loop of $Ca_v2.2$ appears as a particularly interesting structural determinant for supporting G-protein dissociation. First, it contains several $G_{\beta\gamma}$ binding determinants whose functional role remains unclear (12, 15, 23, 34, 53, 54). Second, this loop is known to contribute to fast inactivation (21, 23, 46)) possibly through a hinged lid mechanism that would impede the ion pore (46). Third, some of the residues of the QXXER motif have been found to contribute to inactivation in a voltage-sensitive manner (41). A possible working hypothesis for the contribution of the I–II loop to G-protein regulation can be proposed: i) the channel openings provide an initial destabilizing event favouring G-proteindissociation, and ii) the hinged lid movement of the I–II loop triggered by the inactivation process further accelerates G-protein dissociation through an additional decrease in affinity between $G_{\beta\gamma}$ and the channel.

There is however an alternative possibility based on the expected relationship between channel opening probability and rate of G protein dissociation (48). At the potential at which we performed this study (10 mV), all channel combinations are at their maximal activation (data not shown) and should produce maximal opening probabilities. Nevertheless, we can't rule out that the various β subunits and structural analogues introduce differences in the maximal opening probabilities of the channel thereby explaining differences in the rate of G protein dissociation: e.g. β_{2a} with a lower opening probability and thus slower recovery from inhibition. However, this would imply that anything that leads to a slowing of inactivation kinetics, through a modification of β subunit structure, produces a reduced opening probability. The likelihood of this hypothesis is probably low, but can't be dismissed.

Inactivation differentially affects each characteristic biophysical channel modification induced during G-protein regulation

Since time-dependent G-protein dissociation is responsible for the characteristic biophysical modifications of the channel (48), inactivation, by altering the parameters of the recovery from inhibition, plays a crucial role in the phenotype of G-protein regulation. Two extreme case scenarios were observed. G-protein regulation of slowly inactivating channels, such as $Ca_v2.2/\beta_{1b\ \Delta N}$, induces an important slowing of the activation kinetics, but no or little depolarizing shift of the voltage-dependence of activation and less peak current inhibition. Conversely, faster inactivating channels, such as $Ca_v2.2/\beta_{1b}$, present reduced slowing of activation kinetics, but a greater peak current inhibition and a marked depolarizing shift of the voltage-dependence of activation. These data point to the fact that characteristic biophysical changes of the channel under G-protein regulation should not be correlated with each other. Indeed, an important shift of the time to peak is not necessarily associated with an important depolarizing shift of the voltage-dependence of activation or a greater peak current reduction. It thus seems important to be cautious on the absence of a particular phenotype of G-protein regulation that does not necessarily reflect the lack of direct G-protein inhibition.

Physiological implications of channel inactivation in G-protein regulation

N-type channels are rather heterogeneous by their inactivation properties because of differences in subunit composition (43) or in alternative splicing (5, 28). Very little information is available on the targeting determinants that lead to N-type channel insertion at the synapse. However, a contribution of the β subunits and of specific C-terminal sequences of $Ca_v2.2$ is thought to be involved in the sorting of mature channels (24). An epileptic lethargic phenotype in mouse is known to arise from the loss of expression of the β_4 subunit, which is accompanied by a β subunit reshuffling in N-type channels (9). These animals present an altered excitatory synaptic transmission suggesting the occurrence of a modification in channel composition and/or regulation at the synapse (10). Synaptic terminals that arise from single axons present a surprising heterogeneity in calcium channel composition and in processing capabilities (39). One of the synaptic properties most influenced by calcium channel subtypes is presynaptic inhibition by G-proteins. Evidence has been provided that the extent of N-type current facilitation (hence current recovery from G-protein inhibition) is dependent on both the duration (8) and the frequency of action potentials (AP) (36, 50). Low frequencies of AP produce no or little recovery, whereas high frequency action potentials more dramatically enhance recovery. Hence, slowly inactivating channels should allow much better recovery from G-protein inhibition than fastly inactivating channels, thereby further enhancing the processing abilities of synaptic terminals. In that sense, a model of synaptic integration has been proposed by the group of Dr. Zamponi that would be implicated in short-term synaptic facilitation or depression (6). It should be noted that inactivation of calcium channels does not only rely on a voltage-dependent component, and that other modulatory signals (calcium-dependent inactivation, phosphorylation) need to find a place in the integration pathway.

Conclusion

These data permit a better understanding of the role of inactivation in N-type calcium channel regulation by G-proteins and will call attention to the contribution of the different β subunits in physiological responses at the synapse.

Ackowledgements:

We thank Dr. Pierre Charnet and Dr. Yasuo Mori for providing the cDNAs encoding the rat μ-opioid receptor and the rabbit $Ca_v2.2$ channel, respectively. We are indebted to Dr. Anne Feltz, Dr. Lubica Lacinova, Dr. Michel Vivaudou and Dr. Eric Hosy for critical evaluation of this work. We thank Sandrine Geib for her contribution to the CD8-β_{1b} construct.

Footnotes:

Executive editor: Prof. Dr. Bernd Nilius

The following abbreviations have been used

DAMGO: D-Ala^2, Me-Phe^4, glycinol^5)-Enkephalin
rMOR: Rat μ-opioid receptor
PCR: polymerase chain reaction
RI: Recovery from inhibition
NS: non statistically significant

References:

- 1. Agler HL , Evans J , Tay LH , Anderson MJ , Colecraft HM , Yue DT 2005; G protein-gated inhibitory module of N-type ($Ca_v2.2$) Ca2+ channels. Neuron. 46: 891- 904
- 2. Ahern CA , Sheridan DC , Cheng W , Mortenson L , Nataraj P , Allen P , De Waard M , Coronado R 2003; Ca^{2+} current and charge movements in skeletal myotubes promoted by the β-subunit of the dihydropyridine receptor in the absence of ryanodine receptor type 1. Biophys J. 84: 942- 959
- 3. Artalejo CR , Adams ME , Fox AP 1994; Three types of Ca^{2+} channel trigger secretion with different efficacies in chromaffin cells. Nature. 367: 72- 76
- 4. Bean BP 1989; Neurotransmitter inhibition of neuronal calcium currents by changes in channel voltage dependence. Nature. 340: 153- 156
- 5. Bell TJ , Thaler C , Castiglioni AJ , Helton TD , Lipscombe D 2004; Cell-specific alternative splicing increases calcium channel current density in the pain pathway. Neuron. 41: 127- 138
- 6. Bertram R , Swanson J , Yousef M , Feng ZP , Zamponi GW 2003; A minimal model for G protein-mediated synaptic facilitation and depression. Journal of neurophysiology. 90: 1643- 1653
- 7. Boland LM , Bean BP 1993; Modulation of N-type calcium channels in bullfrog sympathetic neurons by luteinizing hormone-releasing hormone: kinetics and voltage dependence. J Neurosci. 13: 516- 533
- 8. Brody DL , Patil PG , Mulle JG , Snutch TP , Yue DT 1997; Bursts of action potential waveforms relieve G-protein inhibition of recombinant P/Q-type Ca^{2+} channels in HEK 293 cells. J Physiol. 499 : (Pt 3) 637- 644
- 9. Burgess DL , Jones JM , Meisler MH , Noebels JL 1997; Mutation of the Ca^{2+} channel β subunit gene Cchb4 is associated with ataxia and seizures in the lethargic (lh) mouse. Cell. 88: 385- 392
- 10. Caddick SJ , Wang C , Fletcher CF , Jenkins NA , Copeland NG , Hosford DA 1999; Excitatory but not inhibitory synaptic transmission is reduced in lethargic (Cacnb4(lh)) and tottering (Cacna1atg) mouse thalami. Journal of neurophysiology. 81: 2066- 2074
- 11. Canti C , Bogdanov Y , Dolphin AC 2000; Interaction between G proteins and accessory subunits in the regulation of α_{1B} calcium channels in Xenopus oocytes. J Physiol. 527: (Pt 3) 419- 432
- 12. Canti C , Page KM , Stephens GJ , Dolphin AC 1999; Identification of residues in the N terminus of α_{1B} critical for inhibition of the voltage-dependent calcium channel by $G_{\beta\gamma}$. J Neurosci. 19: 6855- 6864
- 13. Chien AJ , Carr KM , Shirokov RE , Rios E , Hosey MM 1996; Identification of palmitoylation sites within the L-type calcium channel β_{2a} subunit and effects on channel function. J Biol Chem. 271: 26465- 26468

- 14. De Waard M , Hering J , Weiss N , Feltz A 2005; How do G proteins directly control neuronal Ca^{2+} channel function?. Trends Pharmacol Sci. 26: 427- 436
- 15. De Waard M , Liu H , Walker D , Scott VE , Gurnett CA , Campbell KP 1997; Direct binding of G-protein βγ complex to voltage-dependent calcium channels. Nature. 385: 446- 450
- 16. De Waard M , Pragnell M , Campbell KP 1994; Ca^{2+} channel regulation by a conserved β subunit domain. Neuron. 13: 495- 503
- 17. Doupnik CA , Pun RY 1994; G-protein activation mediates prepulse facilitation of Ca^{2+} channel currents in bovine chromaffin cells. J Membr Biol. 140: 47- 56
- 18. Dunlap K , Fischbach GD 1981; Neurotransmitters decrease the calcium conductance activated by depolarization of embryonic chick sensory neurones. J Physiol. 317: 519 - 535
- 19. Eppig JJ , Dumont JN 1976; Defined nutrient medium for the in vitro maintenance of Xenopus laevis oocytes. In Vitro. 12: 418- 427
- 20. Feng ZP , Arnot MI , Doering CJ , Zamponi GW 2001; Calcium channel β subunits differentially regulate the inhibition of N-type channels by individual G_{β} isoforms. J Biol Chem. 276: 45051- 45058
- 21. Geib S , Sandoz G , Cornet V , Mabrouk K , Fund-Saunier O , Bichet D , Villaz M , Hoshi T , Sabatier JM , De Waard M 2002; The interaction between the I-II loop and the III-IV loop of $Ca_v2.1$ contributes to voltage-dependent inactivation in a β-dependent manner. J Biol Chem. 277: 10003- 10013
- 22. Herlitze S , Garcia DE , Mackie K , Hille B , Scheuer T , Catterall WA 1996; Modulation of Ca^{2+} channels by G-protein βγ subunits. Nature. 380: 258- 262
- 23. Herlitze S , Hockerman GH , Scheuer T , Catterall WA 1997; Molecular determinants of inactivation and G protein modulation in the intracellular loop connecting domains I and II of the calcium channel α_{1A} subunit. Proc Natl Acad Sci U S A. 94: 1512- 1516
- 24. Herlitze S , Xie M , Han J , Hummer A , Melnik-Martinez KV , Moreno RL , Mark MD 2003; Targeting mechanisms of high voltage-activated Ca^{2+} channels. J Bioenerg Biomembr. 35: 621- 637
- 25. Hille B 1994; Modulation of ion-channel function by G-protein-coupled receptors. Trends Neurosci. 17: 531- 536
- 26. Ikeda SR 1991; Double-pulse calcium channel current facilitation in adult rat sympathetic neurones. J Physiol. 439: 181- 214
- 27. Ikeda SR 1996; Voltage-dependent modulation of N-type calcium channels by G-protein βγ subunits. Nature. 380: 255- 258
- 28. Lin Z , Haus S , Edgerton J , Lipscombe D 1997; Identification of functionally distinct isoforms of the N-type Ca^{2+} channel in rat sympathetic ganglia and brain. Neuron. 18: 153- 166
- 29. Lipscombe D , Kongsamut S , Tsien RW 1989; α-adrenergic inhibition of sympathetic neurotransmitter release mediated by modulation of N-type calcium-channel gating. Nature. 340: 639- 642
- 30. Marchetti C , Carbone E , Lux HD 1986; Effects of dopamine and noradrenaline on Ca^{2+} channels of cultured sensory and sympathetic neurons of chick. Pflugers Arch. 406: 104- 111
- 31. Meir A , Dolphin AC 2002; Kinetics and $G_{\beta\gamma}$ modulation of $Ca_v2.2$ channels with different auxiliary β subunits. Pflugers Arch. 444: 263- 275
- 32. Olcese R , Qin N , Schneider T , Neely A , Wei X , Stefani E , Birnbaumer L 1994; The amino terminus of a calcium channel β subunit sets rates of channel inactivation independently of the subunit's effect on activation. Neuron. 13: 1433- 1438
- 33. Page KM , Canti C , Stephens GJ , Berrow NS , Dolphin AC 1998; Identification of the amino terminus of neuronal Ca2+ channel α_1 subunits α_{1B} and α_{1E} as an essential determinant of G-protein modulation. J Neurosci. 18: 4815- 4824
- 34. Page KM , Stephens GJ , Berrow NS , Dolphin AC 1997; The intracellular loop between domains I and II of the B-type calcium channel confers aspects of G-protein sensitivity to the E-type calcium channel. J Neurosci. 17: 1330- 1338
- 35. Patil PG , de Leon M , Reed RR , Dubel S , Snutch TP , Yue DT 1996; Elementary events underlying voltage-dependent G-protein inhibition of N-type calcium channels. Biophys J. 71: 2509- 2521
- 36. Penington NJ , Kelly JS , Fox AP 1991; A study of the mechanism of Ca^{2+} current inhibition produced by serotonin in rat dorsal raphe neurons. J Neurosci. 11: 3594- 3609
- 37. Qin N , Olcese R , Zhou J , Cabello OA , Birnbaumer L , Stefani E 1996; Identification of a second region of the β-subunit involved in regulation of calcium channel inactivation. Am J Physiol. 271: C1539- 1545
- 38. Qin N , Platano D , Olcese R , Stefani E , Birnbaumer L 1997; Direct interaction of $G_{\beta\gamma}$ with a C-terminal $G_{\beta\gamma}$-binding domain of the Ca^{2+} channel α_1 subunit is responsible for channel inhibition by G protein-coupled receptors. Proc Natl Acad Sci U S A. 94: 8866- 8871
- 39. Reid CA , Bekkers JM , Clements JD 2003; Presynaptic Ca^{2+} channels: a functional patchwork. Trends Neurosci. 26: 683- 687
- 40. Restituito S , Cens T , Barrere C , Geib S , Galas S , De Waard M , Charnet P 2000; The β_{2a} subunit is a molecular groom for the Ca^{2+} channel inactivation gate. J Neurosci. 20: 9046- 9052
- 41. Sandoz G , Lopez-Gonzalez I , Stamboulian S , Weiss N , Arnoult C , De Waard M 2004; Repositioning of charged I–II loop amino acid residues within the electric field by β subunit as a novel working hypothesis for the control of fast P/Q calcium channel inactivation. Eur J Neurosci. 19: 1759- 1772
- 42. Scott RH , Dolphin AC 1990; Voltage-dependent modulation of rat sensory neurone calcium channel currents by G protein activation: effect of a dihydropyridine antagonist. Br J Pharmacol. 99: 629- 630
- 43. Scott VE , De Waard M , Liu H , Gurnett CA , Venzke DP , Lennon VA , Campbell KP 1996; β subunit heterogeneity in N-type Ca^{2+} channels. J Biol Chem. 271: 3207- 3212
- 44. Simen AA , Lee CC , Simen BB , Bindokas VP , Miller RJ 2001; The C terminus of the Ca^{2+} channel α_{1B} subunit mediates selective inhibition by G-protein-coupled receptors. J Neurosci. 21: 7587- 7597
- 45. Stephens GJ , Page KM , Bogdanov Y , Dolphin AC 2000; The α_{1B} Ca^{2+} channel amino terminus contributes determinants for β subunit-mediated voltage-dependent inactivation properties. J Physiol. 525: (Pt 2) 377- 390
- 46. Stotz SC , Hamid J , Spaetgens RL , Jarvis SE , Zamponi GW 2000; Fast inactivation of voltage-dependent calcium channels. A hinged-lid mechanism?. J Biol Chem. 275 : 24575- 24582
- 47. Takahashi T , Momiyama A 1993; Different types of calcium channels mediate central synaptic transmission. Nature. 366: 156- 158
- 48. Weiss N , Arnoult C , Feltz A , De Waard M 2006; Contribution of the kinetics of G protein dissociation to the characteristic modifications of N-type calcium channel activity. Neurosci Res. 56: 332- 343
- 49.. Weiss N , De Waard M 2006; Introducing an alternative biophysical method to analyze direct G protein regulation of voltage-dependent calcium channels. J Neurosci Methods. 10.1016/j.jneumeth.2006.08.010
- 50. Williams S , Serafin M , Muhlethaler M , Bernheim L 1997; Facilitation of N-type calcium current is dependent on the frequency of action potential-like depolarizations in dissociated cholinergic basal forebrain neurons of the guinea pig. J Neurosci. 17: 1625- 1632
- 51. Wu LG , Saggau P 1997; Presynaptic inhibition of elicited neurotransmitter release. Trends Neurosci. 20: 204- 212
- 52. Zamponi GW 2001; Determinants of G protein inhibition of presynaptic calcium channels. Cell Biochem Biophys. 34: 79- 94
- 53. Zamponi GW , Bourinet E , Nelson D , Nargeot J , Snutch TP 1997; Crosstalk between G proteins and protein kinase C mediated by the calcium channel α_1 subunit. Nature. 385: 442- 446
- 54. Zhang JF , Ellinor PT , Aldrich RW , Tsien RW 1996; Multiple structural elements in voltage-dependent Ca^{2+} channels support their inhibition by G proteins. Neuron. 17: 991- 1003

Fig. 1

Illustration of steps leading to the determination of the biophysical parameters of N-type currents regulation by G-proteins, according to (49). **a** Representative $Ca_v2.2/\beta_{1b}$ current traces elicited at 10 mV for control ($I_{Control}$) and DAMGO (I_{DAMGO}) conditions. **b** Subtracting I_{DAMGO} from $I_{Control}$ results in I_{Lost} (blue trace), the evolution of the lost current under G-protein activation. $I_{Control}$ and I_{Lost} are then extrapolated to t = 0 ms (the start of the depolarisation) by fitting traces (red dashed lines) with a single and double exponential, respectively, in order to determine GI_{t_0} , the maximal extend of G-protein inhibition. **c** $I_{DAMGO\ without\ unbinding}$ ($I_{DAMGO\ wo\ unbinding}$, blue trace) represents an estimate of the amount of control current that is present in I_{DAMGO} and is obtained by the following equation: $I_{DAMGO\ without\ unbinding} = I_{Control} \times (1 - (I_{Lost_{t_0}} / I_{Control_{t_0}}))$. **d** Subtracting $I_{DAMGO\ wo\ unbinding}$ from I_{DAMGO} results in $I_{G\text{-}protein\ unbinding\ with\ inactivation}$ (blue trace), the evolution of inhibited current that recovers from G-protein inhibition following depolarisation. **e** $I_{G\text{-}protein\ unbinding\ with\ inactivation}$ is divided by the fit trace (normalized to 1) describing inactivation kinetics of the control current (grey dashed line) in order to reveal the net kinetics of G-protein dissociation ($I_{G\text{-}protein\ unbinding}$, blue trace) from the channels. A fit of $I_{G\text{-}protein\ unbinding}$ (red dashed line) by a mono-exponential decrease provides the time constant τ of G-protein dissociation from the channel. **f** The percentage of recovery from G-protein inhibition (RI, in red) at the end of 500 ms pulse is measured as $RI = (I_{DAMGO} - I_{DAMGO\ wo\ unbinding})/(I_{Control} - I_{DAMGO\ wo\ unbinding}) \times 100$. Arrows indicate the start of the depolarisation.

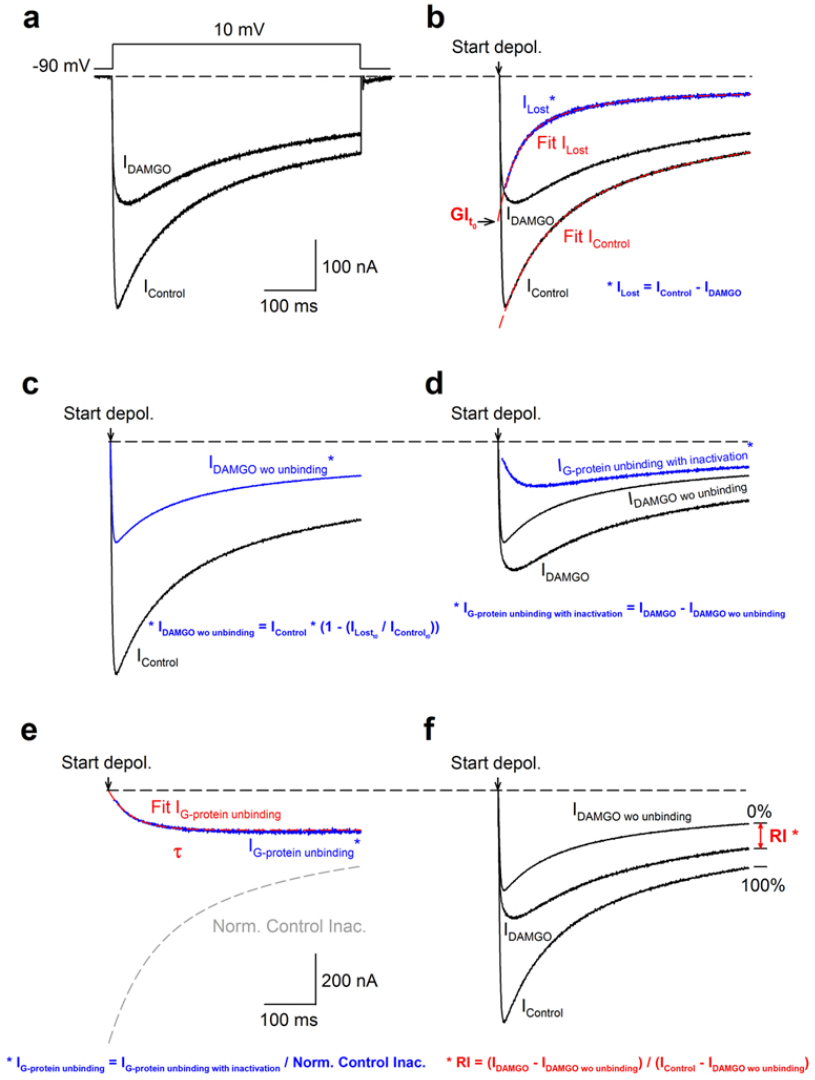

Fig. 2

Maximal G-protein inhibition of N-type currents is independent of the type of β subunits. **a** Representative current traces elicited at 10 mV before ($I_{Control}$) and under 10 μM DAMGO application (I_{DAMGO}) for $Ca_v2.2$ channels co-expressed with the β_{1b}, β_{2a}, β_3 or β_4 subunit (top panel). Corresponding traces allowing the measurement of the maximal DAMGO inhibition at the start of the depolarisation (GI_{t_0}) are also shown for each experimental condition (bottom panel). $I_{Control}$ and I_{Lost} (obtain by subtracting I_{DAMGO} from $I_{Control}$) were fitted by a mono- and a double exponential respectively (red dash lines) in order to better estimate the maximal extent of DAMGO-inhibited current before the start of the depolarisation (GI_{t_0}). The red double arrow indicates the extent the DAMGO-inhibited current at t = 0 ms. Traces were normalized at the maximal value of $I_{Control}$ at t = 0 ms in order to easily compare the extent of current inhibition. b Block diagram representation of GI_{t_0} for each experimental condition. Data are expressed as mean ± S.E.M (in red) for n studied cells.

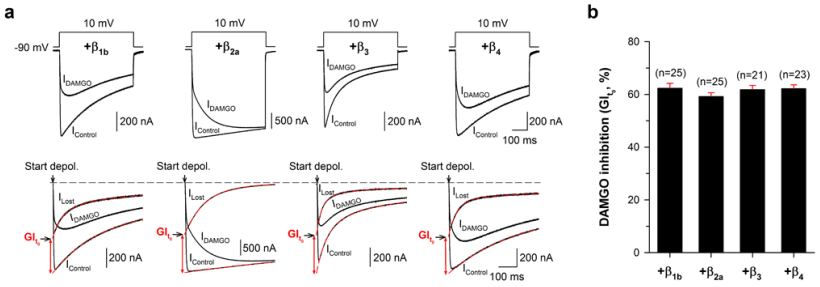

Fig. 3

Influence of β subunits on the recovery of N-type channel inhibition by G-proteins. **a** Representative current traces before ($I_{Control}$) and during application of 10 μM DAMGO (I_{DAMGO}) are shown at 10 mV for $Ca_v2.2$ channels expressed with $β_{1a}$, $β_{2a}$, $β_3$ or $β_4$ subunit (left panel). Corresponding $I_{G\text{-protein unbinding}}$ traces are shown for each condition (middle panel) and were fitted by a mono-exponential decrease (red dashed line) in order to determine the time constant τ of G-protein unbinding from the channel. The arrow indicates the start of the depolarisation. Traces were normalized in order to better compare kinetics. Traces that allowed the measurement of RI values (in red) are also shown for each condition (right panel). **b** Box plot representation of the time constant τ of G-protein unbinding as a function of the type of β subunit co-expressed with $Ca_v2.2$ channels. Number of cells studied is indicated in parentheses. **c** Block diagram representation of RI values measured after 500 ms depolarisation as a function of the type of the β subunit expressed with $Ca_v2.2$ channels. Data are expressed as mean ± S.E.M (in red) for n studied cells. Statistical t-test: NS, none statistically significant; *, p ≤ 0.05; ** p ≤ 0.01; ***, p ≤ 0.001.

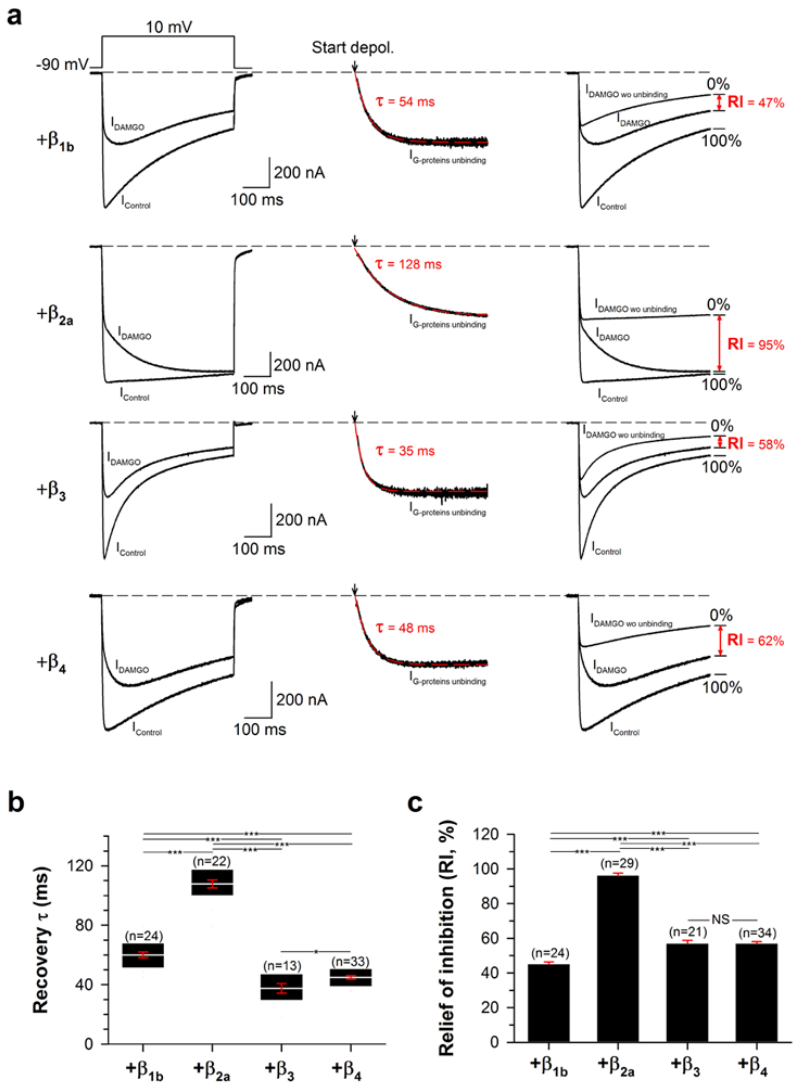

Fig. 4

Slowing of inactivation kinetics by N-terminal truncated β_{1b} subunit modifies recovery of N-type currents inhibition by G-proteins. **a** Representative current elicited by a step depolarisation at 10 mV for $Ca_v2.2$ channels co-expressed with the wild-type β_{1b} subunit or with the N-terminal truncated $\beta_{1b\ \Delta N}$ subunit. Current traces were normalized to facilitate comparison of the kinetics and extent of inactivation. **b** Block diagram representation of the extent of inactivated current after 500 ms depolarisation. **c** Representative current traces before ($I_{Control}$) and during application of 10 μM DAMGO (I_{DAMGO}) are shown at 10 mV for $Ca_v2.2$ channels co-expressed with the wild-type β_{1b} subunit or with the truncated $\beta_{1b\ \Delta N}$ subunit (left panel). Corresponding normalized $I_{G\text{-protein unbinding}}$ traces fitted by a mono-exponential decrease (red dashed line) are shown for each condition (middle panel). The arrow indicates the start of the depolarisation. The black dotted line represents the $Ca_v2.2/\beta_{1b}$ channel condition shown for comparison. Corresponding traces allowed the measure of RI values (in red) are also shown for each experimental condition (right panel). **d** Box plot representation of time constants τ of recovery from G-protein inhibition at 10 mV for each experimental condition. **e** Block diagram representation of RI values after 500 ms depolarisation at 10 mV for each experimental condition. Data are expressed as mean ± S.E.M (in red) for n studied cells. Statistical t-test: ***, $p \leq 0.001$.

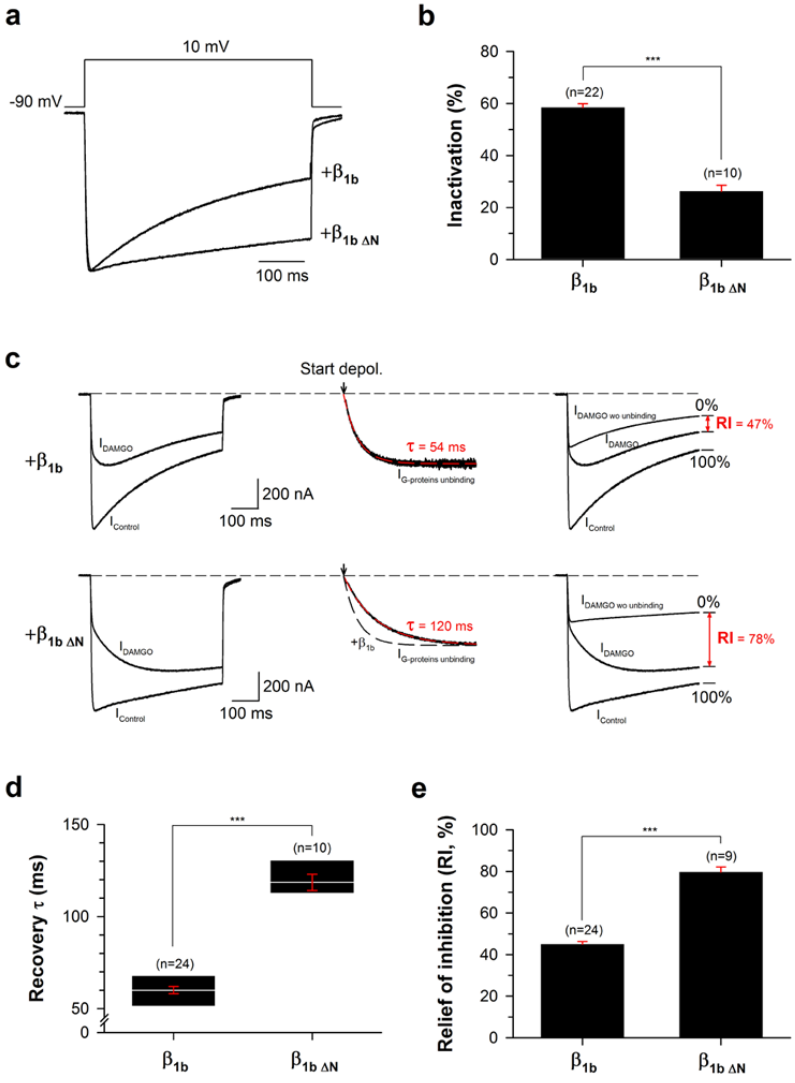

Fig. 5

Slower inactivation kinetics induced by N-terminal truncated β_3 subunit also modifies recovery of N-type current inhibition by G-proteins. Legends as in Fig. 4 but for cells expressing $Ca_v2.2$ channels in combination with the wild-type β_3 subunit or with the N-terminal truncated β_3 Δ_N subunit. Data are expressed as mean ± S.E.M (in red) for n studied cells. Statistical t-test: **, p ≤ 0.01; ***, p ≤ 0.001.

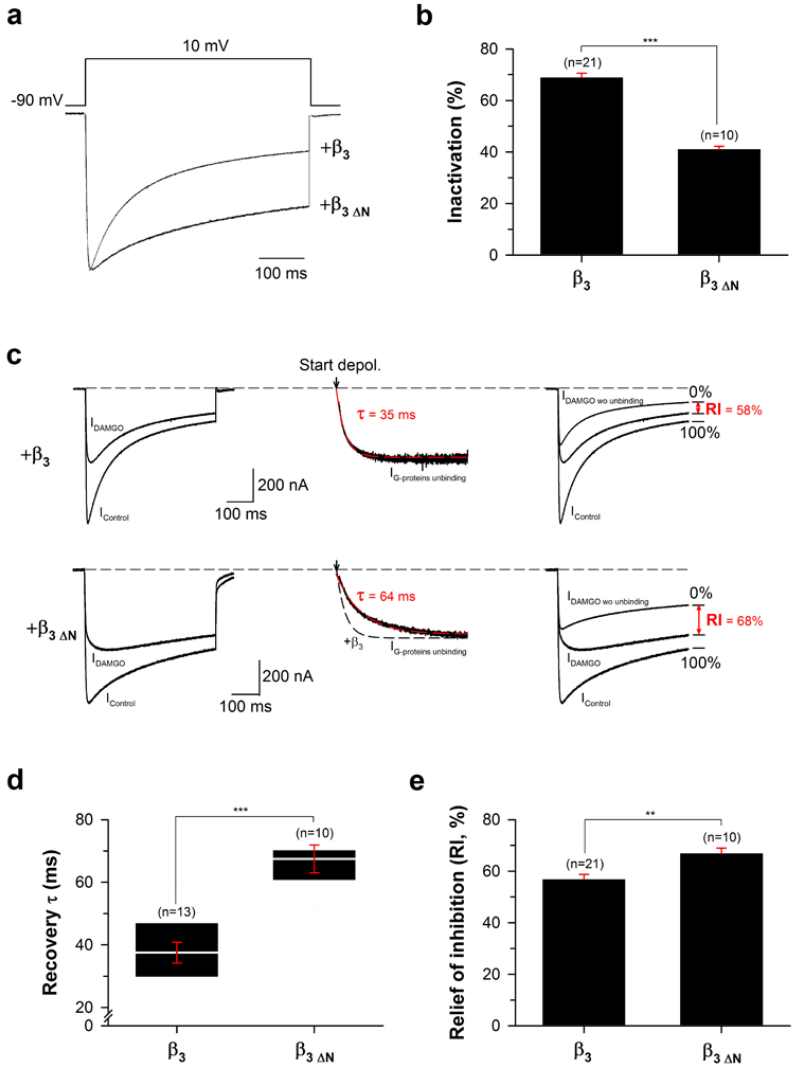

Fig. 6

Slowing of inactivation kinetics by membrane anchoring of β_{1b} subunit modifies recovery of N-type current inhibition by G-proteins. Legends as in Fig. 4 but for cells expressing $Ca_v2.2$ channels in combination with the wild-type β_{1b} subunit or with the membrane-linked CD8≤β_{1b} subunit. Data are expressed as mean ± S.E.M (in red) for n studied cells. Statistical t-test: ***, p ≤ 0.001.

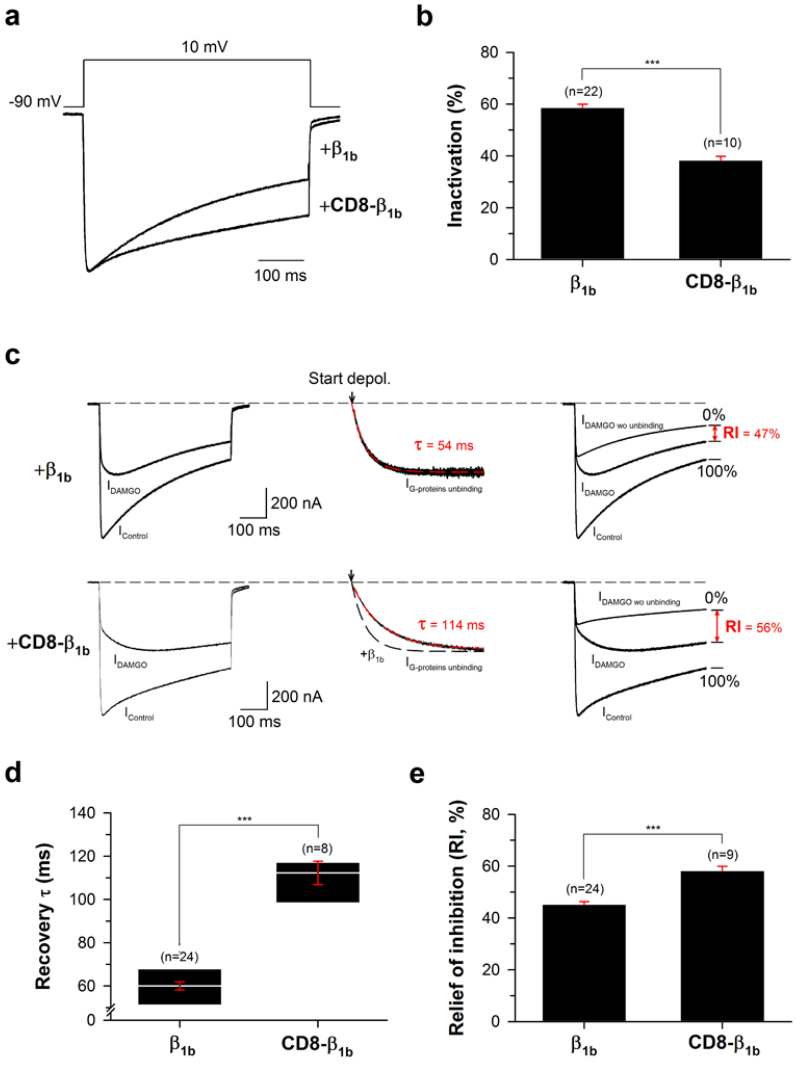

Fig. 7

The extent of N-type channel inactivation correlates with the extent of current recovery from G-protein inhibition. **a** An example of the influence of membrane potential values on the time constant τ of current recovery from G-protein inhibition is shown for $Ca_v2.2/\beta_{1b}$ channels. Normalized $I_{G\text{-protein unbinding}}$ traces fitted by a mono-exponential decrease (red dashed line) are shown for a range of potentials from 0 to +40 mV (left panel). The arrow indicates the start of the depolarisation. Traces were superimposed to facilitate kinetic comparisons. Corresponding voltage-dependence of the time constant τ of current recovery from G-protein inhibition (n=13) is shown (middle panel). Data are expressed as mean ± S.E.M (in red) and were fitted with by a sigmoid function. Scheme illustrating normalized $I_{G\text{-protein unbinding trace}}$ for a define time constant τ of 50 ms ± 5 ms (red and black lines respectively) (right panel). Grey area represents the accepted variation in τ values (± 10%) for the incorporation of current traces in our subsequent analyses. The arrow indicates the virtual start of the depolarisation. **b** Representative normalized current traces before ($I_{Control}$) and under 10 μM DAMGO application (I_{DAMGO}) for $Ca_v2.2$ expressed in combination with β_{2a}, β_4 or β_{1b} subunit at +20 mV, +10 mV et +10 mV respectively (left panel). Traces were selected on the basis of the measured recovery G-protein inhibition time constant τ (between 45 and 55 ms). Corresponding traces allowing the measurement of RI values (in red) after a 500 ms depolarisation (right panel). The grey area represents the extent of current inactivation during a 500 ms depolarisation. **c** Scattered plot representation of RI values after a 500 ms depolarisation as a function of the extent of inactivation. Values are shown for various $Ca_v2.2/\beta$ combinations (n = 62) showing a time constant τ of recovery from G-protein inhibition of 50 ms ± 5 ms independently of the test potential. Fitting these values by a linear curve provided a linear regression coefficient of −0.768 which is statistically significant at $p < 0.001$ (Spearman Rank Order correlation test).

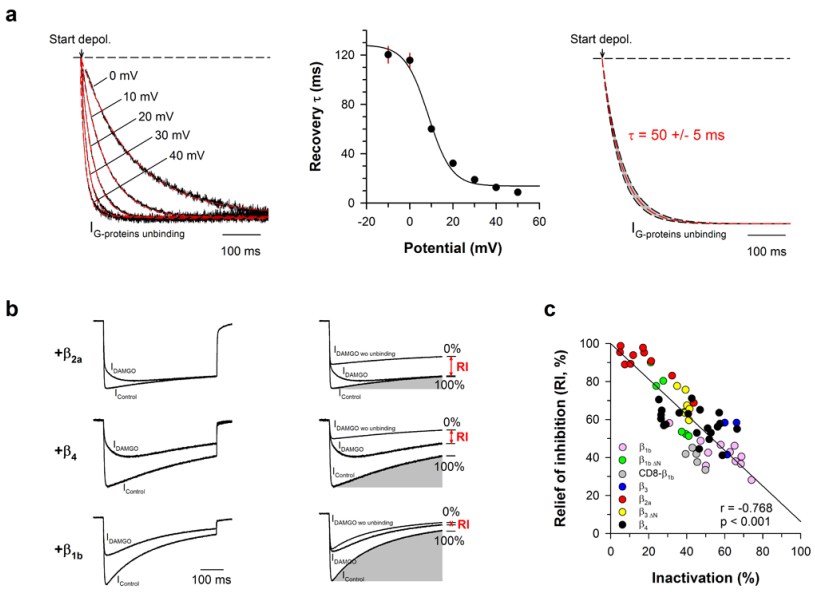

Fig. 8

Effect of channel inactivation on characteristic biophysical changes induced by G- protein activation. Representative current traces before ($I_{Control}$) and under 10 μM DAMGO application (I_{DAMGO}) as well as corresponding traces allowing the measurement of RI values are shown for $Ca_v2.2/\beta_{1b}$ (**a**) and $Ca_v2.2/\beta_{1b\ \Delta N}$ (**b**) at various membrane potentials illustrating DAMGO effects on channel activation kinetics and current recovery from G-protein inhibition in two conditions of channel inactivation. Arrows indicate the time to peak of the currents for control and DAMGO conditions. The time to peak of DAMGO-inhibited currents (I_{DAMGO}) has been indicated also on RI traces (arrows in lower panels). Double arrows indicate the extent of current recovery from G-protein inhibition at these time points (RI_{peak}). **c** Box plot representation of the shift of the current time to peak induced by DAMGO application for $Ca_v2.2/\beta_{1b}$ channels (green boxes, n=14) and $Ca_v2.2/\beta_{1b\ \Delta N}$ channels (blue boxes, n=10) as a function of membrane potential. **d** Histogram representation of RI_{peak} values at the peak of DAMGO currents (I_{DAMGO}) for $Ca_v2.2/\beta_{1b}$ channels (green bars, n=14) and $Ca_v2.2/\beta_{1b\ \Delta N}$ channels (blue bars, n=10) as a function of membrane potential. Current-voltage relationship (I/V) were performed for $Cav2.2/\beta_{1b}$ channels (green plots, n = 13) (**e**) and $Ca_v2.2/\beta_{1b\ \Delta N}$ channels (blue plots, n = 10) (**f**) for control (circle symbol) and DAMGO-inhibited (triangle symbols) currents measured at their peak. Data were fitted with a modified Boltzmann equation as described in Materials and Methods section. Insert represents the shift of the half maximum current activation potential ($V_{1/2}$) induced by DAMGO application for $Ca_v2.2/\beta_{1b}$ (green box, n = 13) and $Ca_v2.2/\beta_{1b\ \Delta N}$ channels (blue box, n = 10). Data are expressed as mean ± S.E.M (in red) for n studied cells. Statistical t-test: NS, none statistically significant; *, p ≤ 0.05; ** p ≤ 0.01; ***, p ≤ 0.001.